

Structural control of Jurassic aquifer geometry in the tabular Middle Atlas Morocco

Soukaina Mouljebouj^{1*}, Mohamed Saadi¹, Smail Souiri², Imane Kounti¹, Wiame El moutchou¹

¹Geosciences laboratory, Department of Geology, Faculty of Sciences, Mohammed V University in Rabat, 4 Avenue Ibn Batouta, B.P. 1014-Morocco; soukainamouljebouj@gmail.com (S.M.) m-saadi@um5r.ac.ma (M.S.) wiame17el@gmail.com (W.E.) imanekounti1994@gmail.com (I.K.).

²Geophysics and Natural Hazards Laboratory, Scientific Institute, Mohammed V University in Rabat, 4 Avenue Ibn Batouta, B.P. 1014-Morocco; smail.souiri@um5r.ac.ma (S.S.).

Abstract: This study aims to delineate the geometry of the Jurassic carbonate aquifer in the Agourai region (Tabular Middle Atlas, Morocco) and to understand the structural controls that influence groundwater flow and storage. An integrated approach was adopted, combining remote sensing techniques with subsurface geological data. Tectonic lineaments were extracted from Landsat 8 OLI satellite images using Principal Component Analysis (PCA), directional Sobel filters, and Gram-Schmidt fusion. These results were then correlated with lithological and structural data from hydrogeological borehole logs to build a three-dimensional geometric model of the aquifer. The analysis identified 1,248 lineaments, revealing a structural framework dominated by NE-SW (45%) and E-W (30%) trending fault systems. Drilling data confirmed that these structures act as major drains, creating a series of horsts and grabens. Aquifer thickness varies significantly across these faults, from 78 meters near the Timelouka fault to a maximum of 180 meters in the depocenter of the Agourai basin. The combined PCA and Sobel method proved most effective, achieving a geological compliance rate of 90.6%. The main limitations of the study are the spatial resolution of satellite imagery (15-30 meters), which may not detect smaller fractures, and the uneven distribution of drilling data. Future research should incorporate high-resolution geophysical surveys to refine the model. The resulting structural map serves as a predictive tool for groundwater exploration, highlighting areas with high potential for future water drilling. This provides a practical guide for the sustainable management of water resources in this semi-arid region. This study is the first in the Agourai region to quantitatively link remotely detected surface lineaments with the geometry of the subsurface aquifer. Its originality lies in demonstrating that NE-SW trending faults are the main control on aquifer thickness, offering a new hydrogeological framework for the Tabular Middle Atlas.

Keywords: Agourai, Middle Atlas, Boreholes, Fractured aquifers, Lineaments, PCA, Remote sensing, Sobel.

1. Introduction

Sustainable management of groundwater resources is a major strategic issue for semi-arid regions, particularly in Morocco where increasing demand places considerable pressure on aquifer systems. Jurassic carbonate aquifers, in particular, represent important potential reservoirs due to their fracture porosity and karstification. However, their effective exploitation is directly conditioned by a precise understanding of their geometry and the tectonic structures that govern groundwater flow. In this context, the Tabular Middle Atlas region, characterized by these formations, constitutes a priority study area for the development of new hydrogeological exploration strategies.

The geological framework of the Tabular Middle Atlas has been the subject of several fundamental studies (e.g., [1, 2]) which described a Hercynian basement overlain by a Meso-Cenozoic cover. Regional tectonics are marked by inherited fault systems, mainly NE-SW and NW-SE oriented,

reactivated during Alpine phases. More recent studies have used remote sensing or geophysics for regional lineament mapping [3] confirming the influence of these major structural directions. However, these works have often been limited to a surface analysis or a general tectonic description.

Despite these advances, a significant gap persists in understanding the direct relationship between surface lineaments and the three-dimensional geometry of the Jurassic aquifer at depth. Most previous studies dissociate surface structural analysis from quantitative hydrogeology. Consequently, the precise impact of faults (orientation, density) on aquifer thickness variations and on the location of maximum productivity zones remains poorly constrained. This lack of direct correlation between remote sensing data and drilling data constitutes a major obstacle to the development of reliable predictive hydrogeological models for the Agourai region.

To fill this gap, the main objective of this study is to characterize the structural control on the geometry of the Jurassic aquifer in the Agourai plateau. To achieve this objective, specific goals have been set: (1) extract and statistically analyze tectonic lineaments from Landsat 8 satellite images; (2) correlate these surface structures with lithological and structural data from hydrogeological boreholes; and (3) produce a conceptual model of the aquifer geometry that explains the distribution of thicknesses and identifies the most favorable areas for groundwater accumulation.

2. Materials and Methods

2.1. Study Area

The study area is centered on the Agourai plateau, located in the northwestern part of the Tabular Middle Atlas of Morocco (Figure 1). Geologically, this plateau is a relatively undeformed structure, characterized by a Meso-Cenozoic sedimentary series unconformably overlying a folded Paleozoic basement [4]. The main aquifer system, which is the subject of this study, is hosted in the Jurassic carbonate formations (limestones and dolomites). These formations, although competent, are intensely affected by a dense network of faults and fractures inherited from the complex tectonic history of the region, making them a fractured reservoir of great hydrogeological interest.

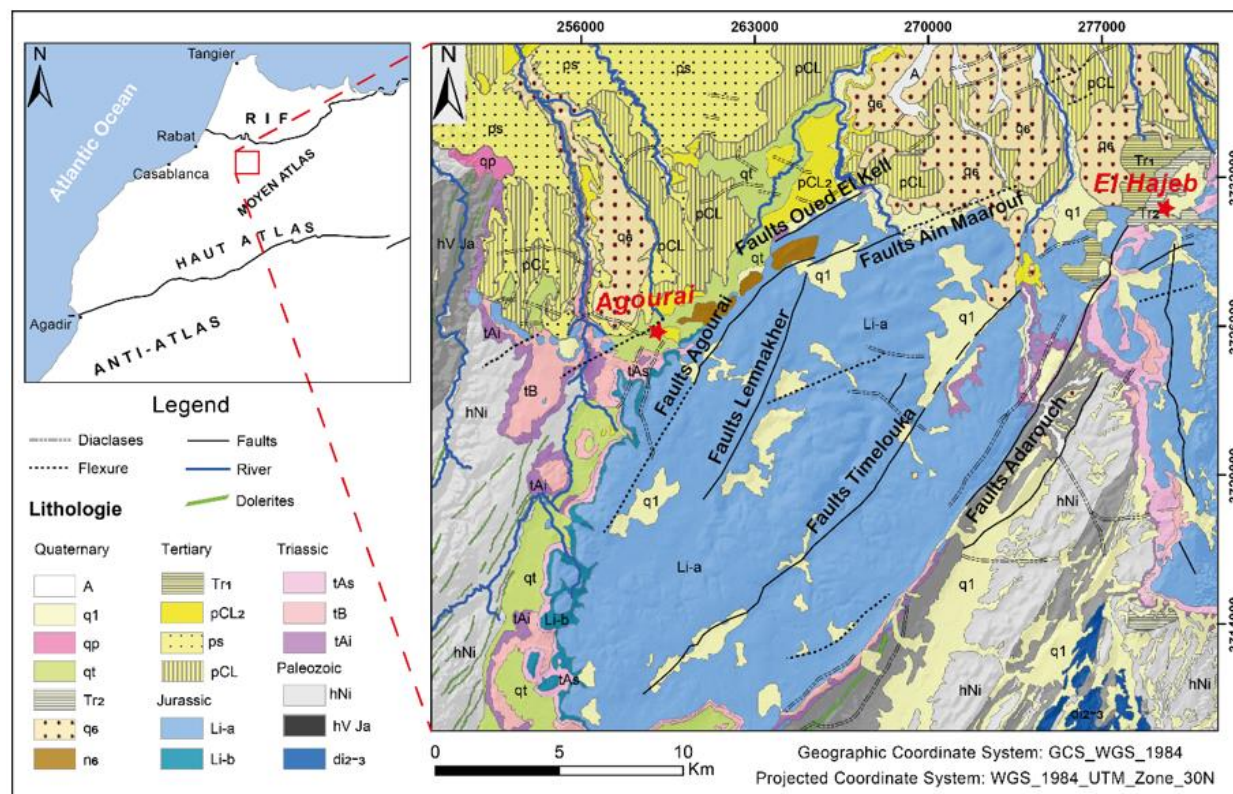


Figure 1.

Geological map of the Agourai plateau. 1: present and recent alluvium; 2: soltanian limons; 3: soils established on Paleozoic terrains; 4: soils established on Triassic basalts and clays; 5: travertine upper levels; 6: ancient silts of the sais; 7: sandy marl; 8: travertine lower levels or pink travertine; 9: long lacustrine limestone; 10: sands and sandstones; 11: lateral facies of lacustrine white clay; 12: yellow marl; 13: dolomitic dolomites and limestones; 14: red or purplish upper clays; 15: doleritic basalts; 16: red or purplish lower clays; 17: alternating sandstones and pelites; 18: alternating shales and turbiditic brown sandstones; 19: alternating shale and sandstone.

The Tabular Middle Atlas constitutes one of the two main structural domains of the Middle Atlas, along with the Folded Domain located farther southeast. The Agourai region, in the northwestern Middle Atlas, belongs to this tabular domain, characterized by a relatively undeformed sedimentary cover resting on a Hercynian basement [1, 4]. This sector is distinguished by a stack of Mesozoic to Cenozoic sedimentary formations arranged in structural tables, reflecting a geodynamic evolution marked by multiple tectonic and sedimentary phases [5].

Tectonically, the Tabular Middle Atlas lies at the interface between the Paleozoic basement of the Moroccan Central Massif to the north and the Folded Domain to the south [6]. It is mainly structured by a system of sub-meridional faults (NNE–SSW to NE–SW), inherited from Hercynian phases and reactivated during the Alpine episodes [2]. The Agourai region is thus affected by a series of normal and strike-slip faults that control both structural styles and sedimentation [5]. The lineaments observed in this region are often associated with these major tectonic structures, some of which act as zones of weakness favoring fluid circulation [6]. This tectonic setting makes the Agourai sector particularly interesting for structural studies using remote sensing, due to the clarity of lineaments visible on satellite imagery.

2.2. Data Acquisition and Preparation

To carry out this study, a multi-source approach was adopted, based on three complementary types of data:

Satellite data: A Landsat 8 OLI/TIRS satellite image was chosen. This sensor is particularly suitable for geological analysis for several reasons: its spatial resolution of 30 m for multispectral bands and 15 m for the panchromatic band is an excellent compromise for regional-scale analysis, allowing the detection of structures from several hundred meters to several kilometers. In addition, its spectral richness is essential for lithological discrimination and contrast enhancement.

Drilling data: Data from 12 hydrogeological boreholes were collected. These data, from public archives and previous field campaigns, are crucial because they provide the only “ground truth” on subsurface geology. Each borehole log provided essential information: the succession of geological layers (lithology), the exact depth of the top and bottom of the Jurassic aquifer, and indications of highly fractured zones (via circulation losses or core descriptions). The location of these boreholes is shown in Figure 2.

Cartographic data: The geological map of Morocco at 1:500,000 scale served as a fundamental reference document. It was used to validate the nature and orientation of the major tectonic features identified by remote sensing and to ensure the consistency of our interpretations with the known regional geological framework.

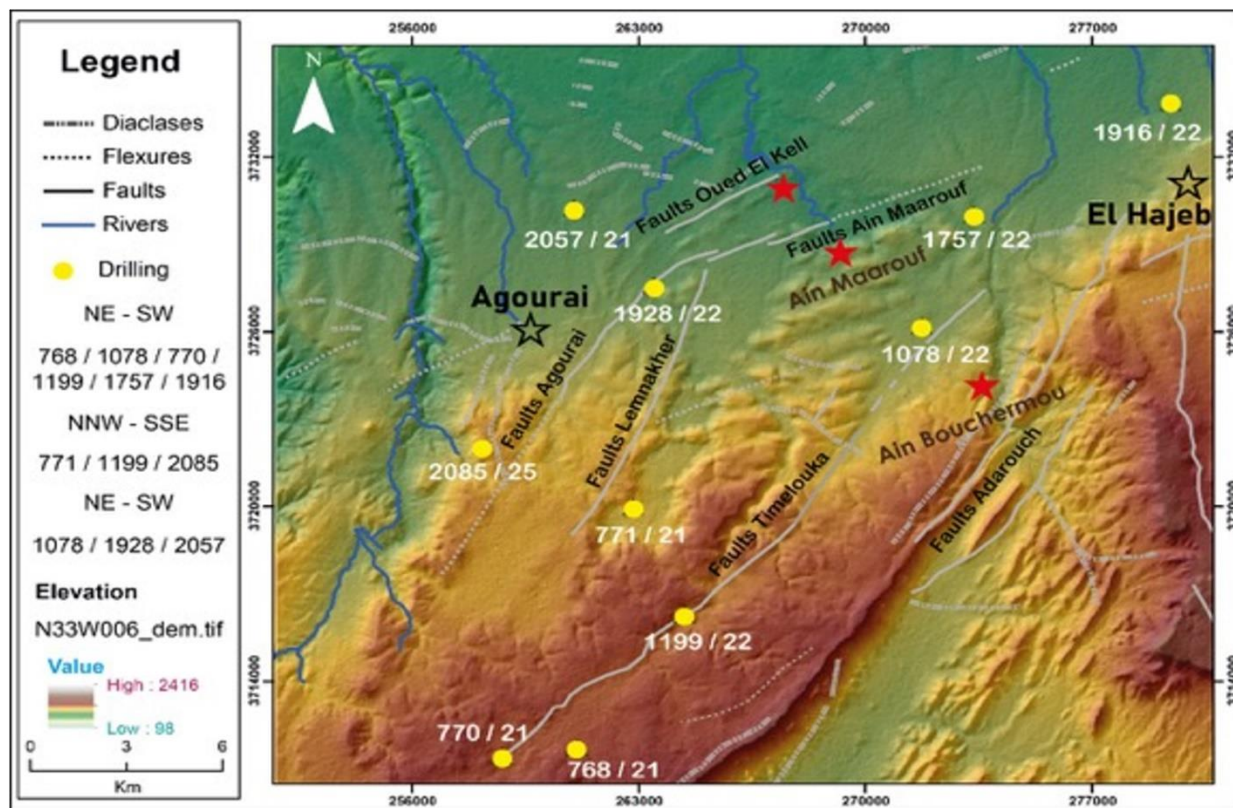


Figure 2.

DEM of the Agourai plateau showing the location of the hydrogeological boreholes.

2.3. Satellite Image Processing and Lineament Extraction

The image processing protocol aimed to enhance structural features that are barely visible to the naked eye. It unfolded in four sequential steps:

1. Preprocessing: This step is fundamental to ensure the reliability of the analyses. Radiometric corrections were applied to convert raw digital values into reflectance, and atmospheric corrections (via the DOS1 method) were used to minimize the effects of haze and atmospheric scattering that can obscure ground details [7, 8]. Figure 3 illustrates the improvement in image quality after correction.

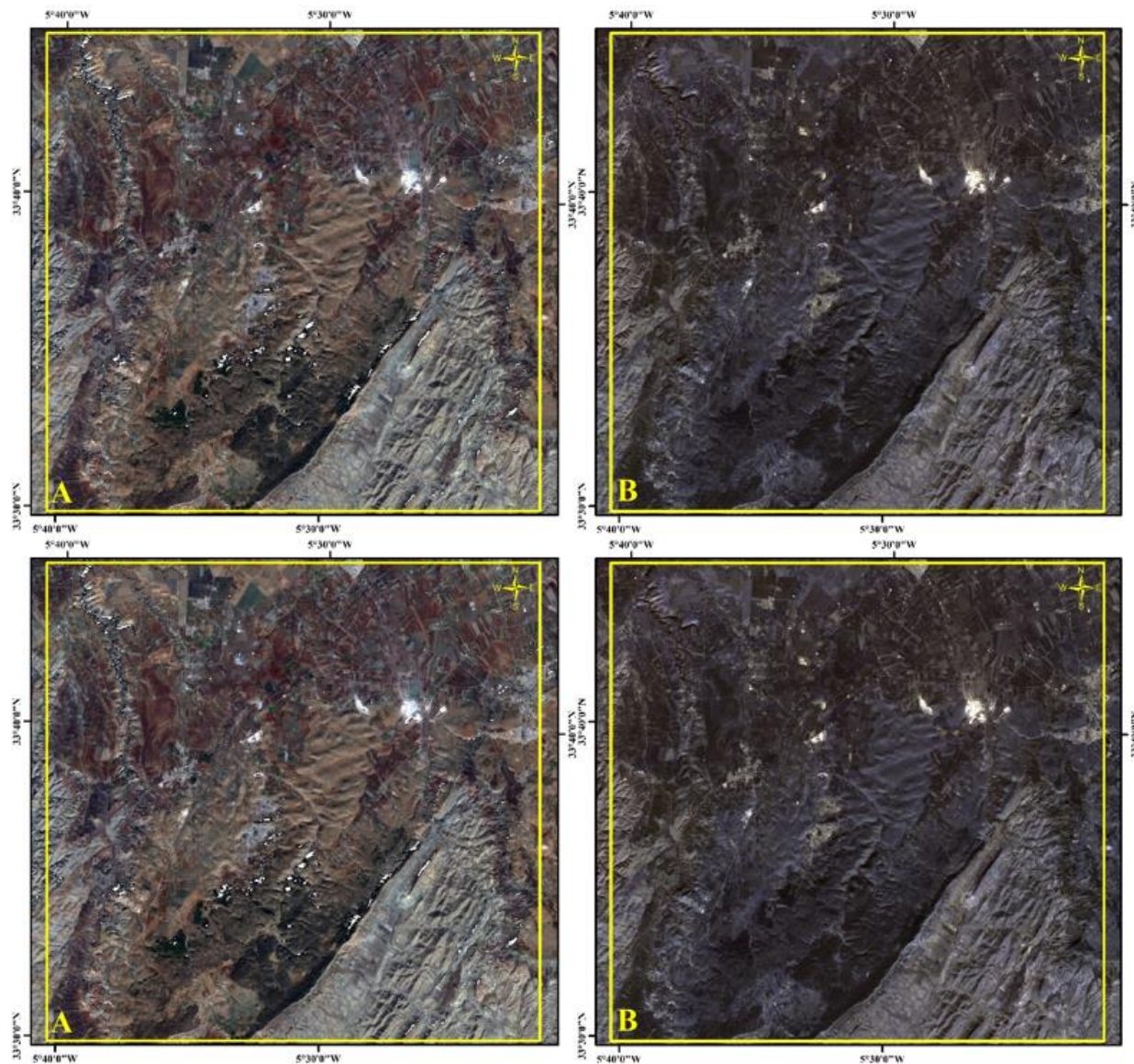


Figure 3.

Atmospheric and radiometric correction applied to a raw Landsat 8 OLI image.

Note: A: Raw image; B: Corrected image.

2. Resolution Enhancement (Pan-sharpening): To benefit from both the color information of the multispectral bands (30 m) and the spatial detail of the panchromatic band (15 m), image fusion using the Gram-Schmidt method was performed. This technique is known for best preserving

spectral fidelity while significantly improving spatial resolution, a major asset for precise lineament delineation [9]. The result is a 15 m resolution color image (Figure 4).

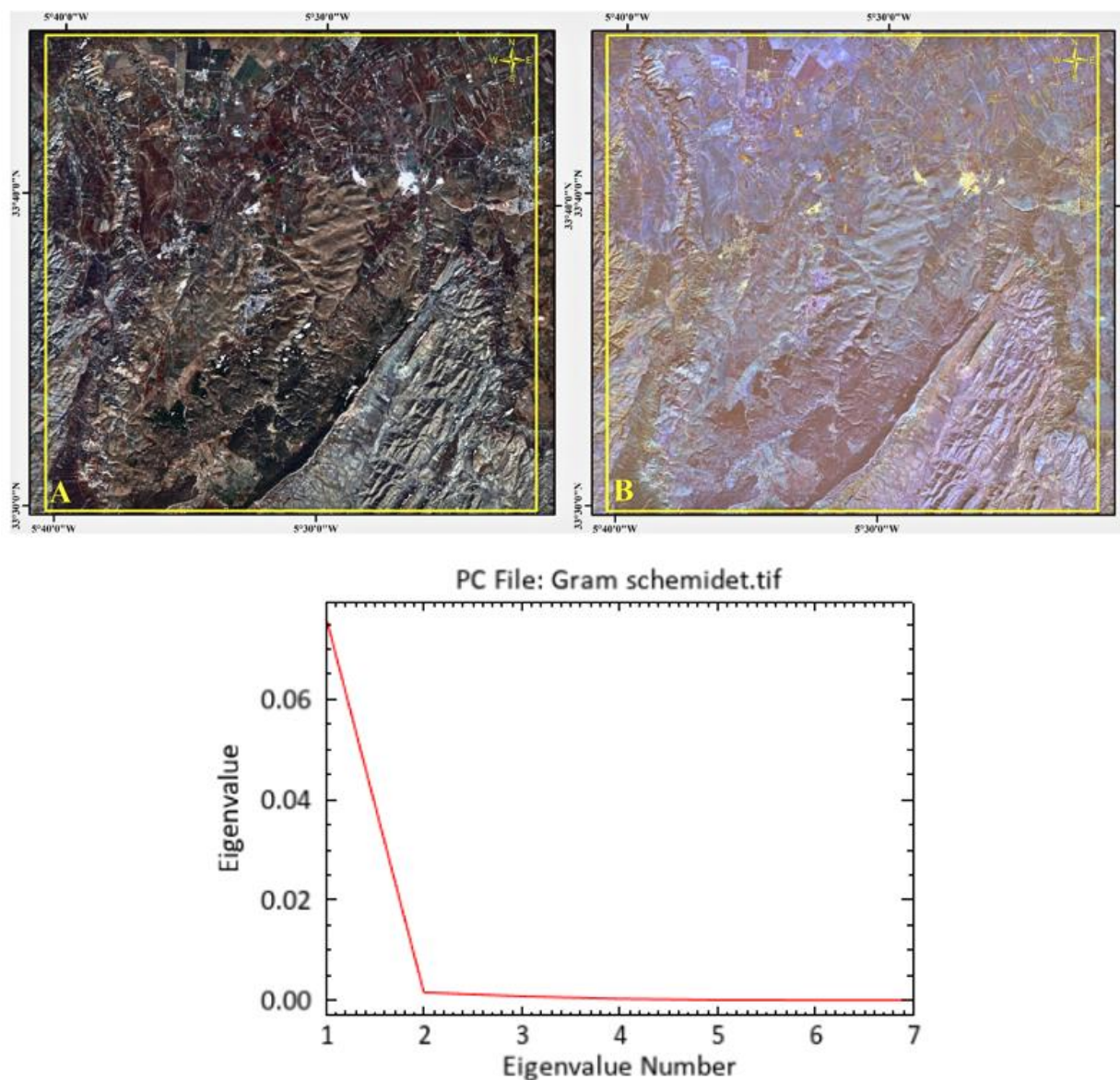


Figure 4.
Result of Gram-Schmidt fusion and Envi Plot.

3. Edge Enhancement: Two complementary techniques were employed. On the one hand, Principal Component Analysis (PCA) was applied to decorrelate spectral bands and concentrate structural information in the first components [10]. On the other hand, directional Sobel filters were applied to the fused image in four directions (N-S, E-W, NE-SW, NW-SE). Each filter acts as a revealer, accentuating alignments perpendicular to its direction [11]. Figure 5 shows an example of an image processed by these filters.

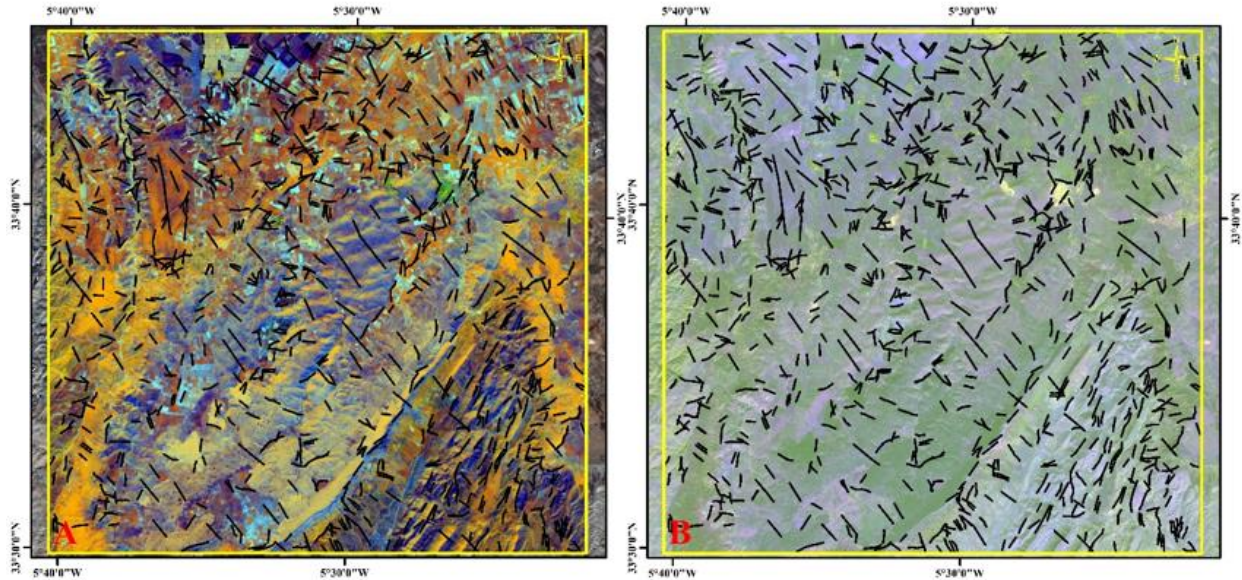


Figure 5.
Sobel-filtered and PCA-enhanced images.

4. **Extraction and Digitization:** Lineaments (topographic, hydrographic, or tonal alignments) were manually digitized on-screen from the various enhanced images. This visual approach, although subjective, allows the operator to use their geological expertise to distinguish tectonic structures from artifacts (roads, plot boundaries). To minimize subjectivity, a validation criterion was applied: a lineament was retained only if it was identifiable on at least two differently processed.

2.4. Drilling Data Analysis and Correlation

This step enabled us to move from 2D (lineament map) to 3D (aquifer geometry). For each borehole, the thickness of the Jurassic aquifer was calculated by subtracting the depth of its wall from that of its roof. The boreholes were then projected onto three transects (NE-SW, NW-SE, and NNW-SSE) chosen to be perpendicular to the main fault families. Correlation sections (Figure 6) were constructed by linking lithological units from borehole to borehole. These sections enable us to directly visualize the vertical offsets induced by the faults and quantify their impact on the thickness of the aquifer.

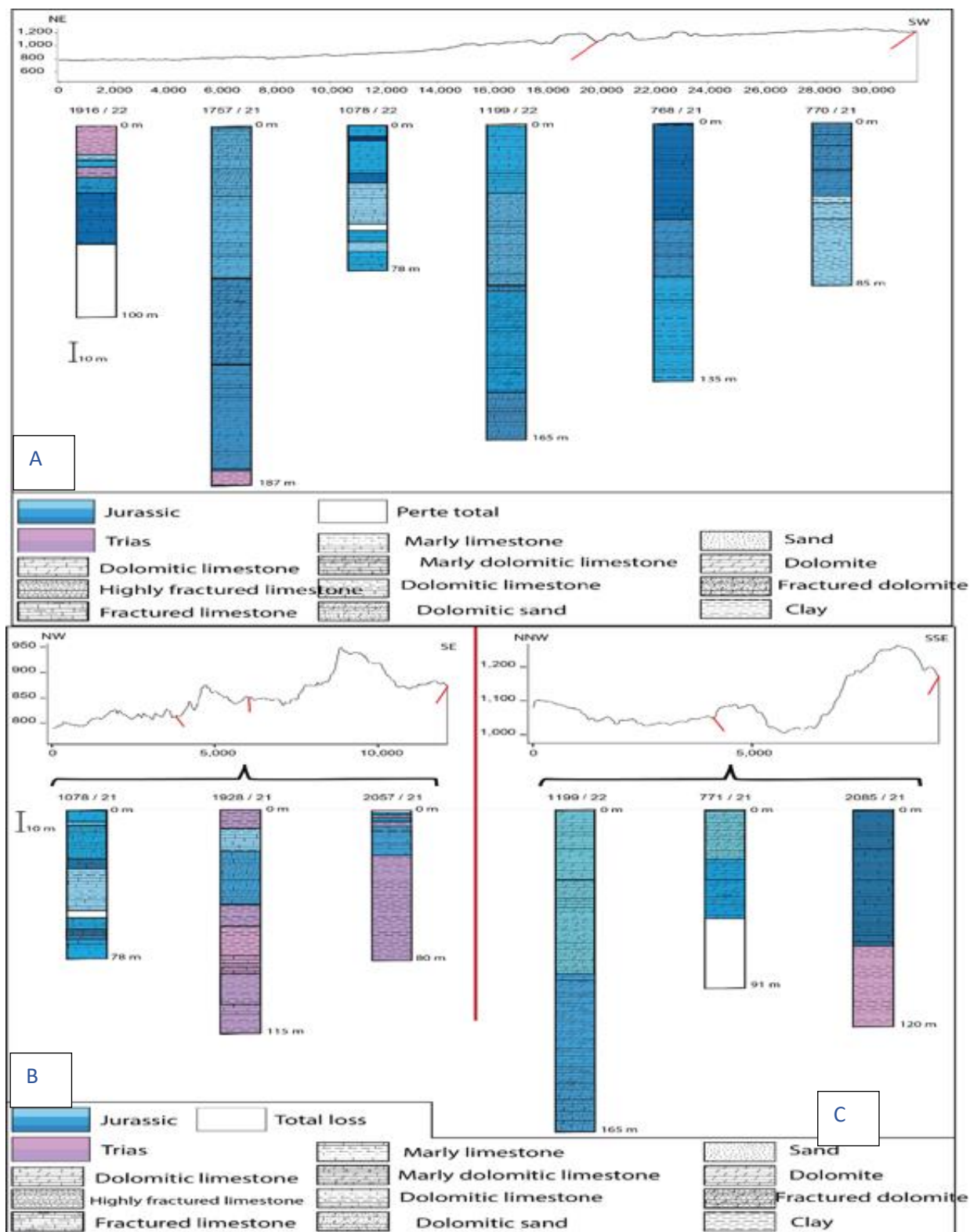


Figure 6.
Correlation between borehole logs along three directions: NE-SW, NW-SE, and NNW-SSE.

2.5. Statistical Analysis and Validation

Once the database of 1,248 lineaments was compiled, a statistical analysis was conducted to extract quantitative information. The length and azimuth of each lineament were calculated. These data were used to generate rose diagrams (directional roses), which are a standard tool for visualizing the frequency of orientations and identifying dominant structural families. The final validation of the lineament map was performed by comparing it with fault measurements taken in the field (during previous campaigns) and with the major structures of the geological map, confirming the relevance of the approach [12, 13].

3. Results

3.1. Lineament Mapping and Statistical Analysis

In accordance with the methodology described (section 2.3), the application of image processing techniques allowed the extraction of a total of 1,248 lineaments across the study area. The resulting map (Fig. 7), superimposed on a false-color composite image, illustrates the spatial distribution and density of these structures. A notable concentration of lineaments is observed in the Jurassic carbonate outcrops, which form the main reliefs of the region. The fracturing density appears lower in Quaternary cover areas, such as alluvial plains, where structures are masked.

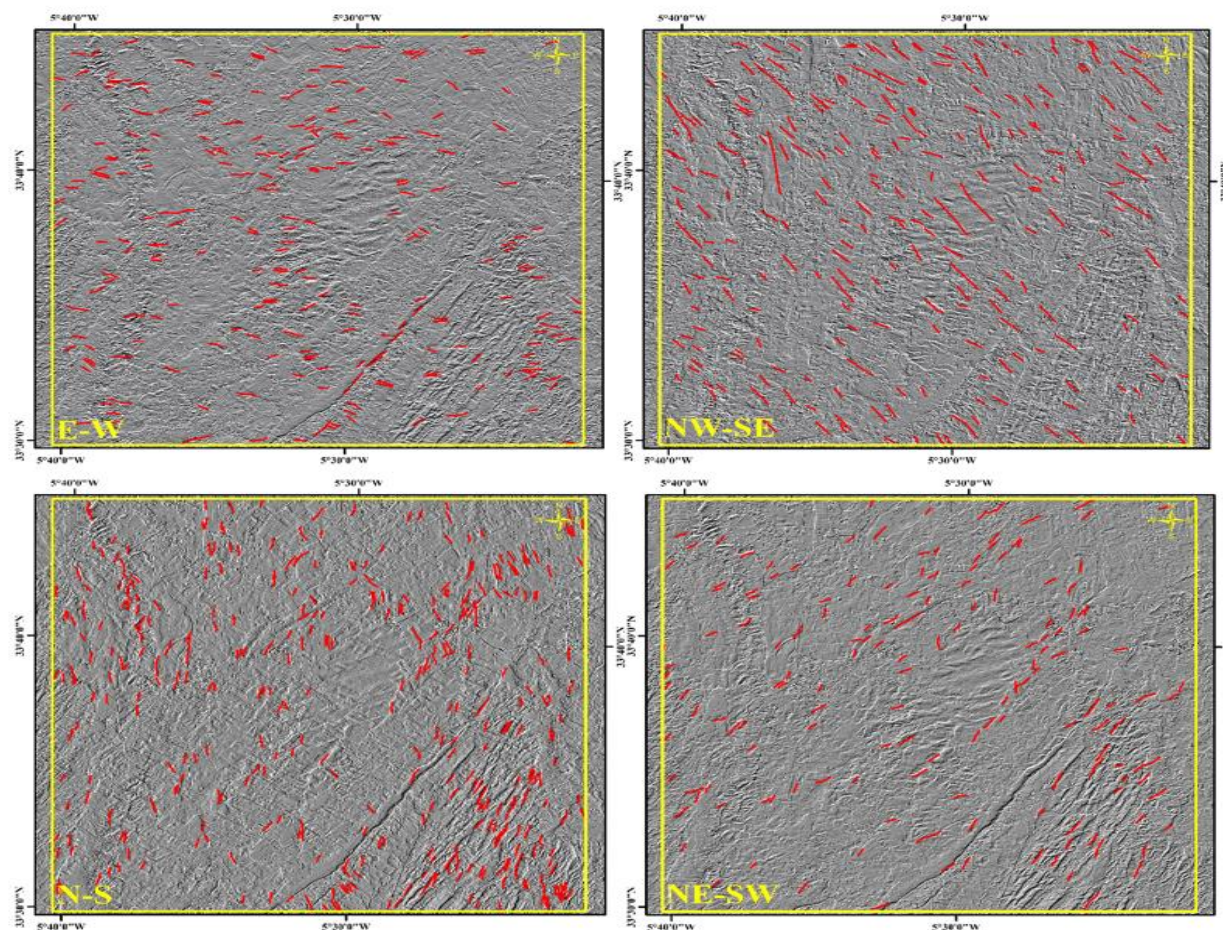


Figure 7.

Map of lineaments overlaid on the Landsat image processed with the four directional Sobel filters.

The statistical analysis of the orientations of these lineaments, summarized in the rose diagrams (Figure 8), reveals a very clear structural organization. The directional rose diagram of all lineaments (Figure 8E) highlights four main families, hierarchical by order of importance:

1. A NE-SW family, which is the most dominant, representing 45% of the total lineament population.
2. A very significant E-W to ENE-WSW family, accounting for 30% of the structures.
3. A NW-SE family, less represented but well-defined, with 15% of the lineaments.
4. A N-S family, which is the most discreet.

The comparison of the performance of the different extraction techniques (Figure 8F for PCA alone vs Figure 8E for the combined method) confirms that the integrated approach (PCA + Sobel filters) allowed for the capture of a more complete and reliable structural signal, in agreement with the known tectonic structures of the region.

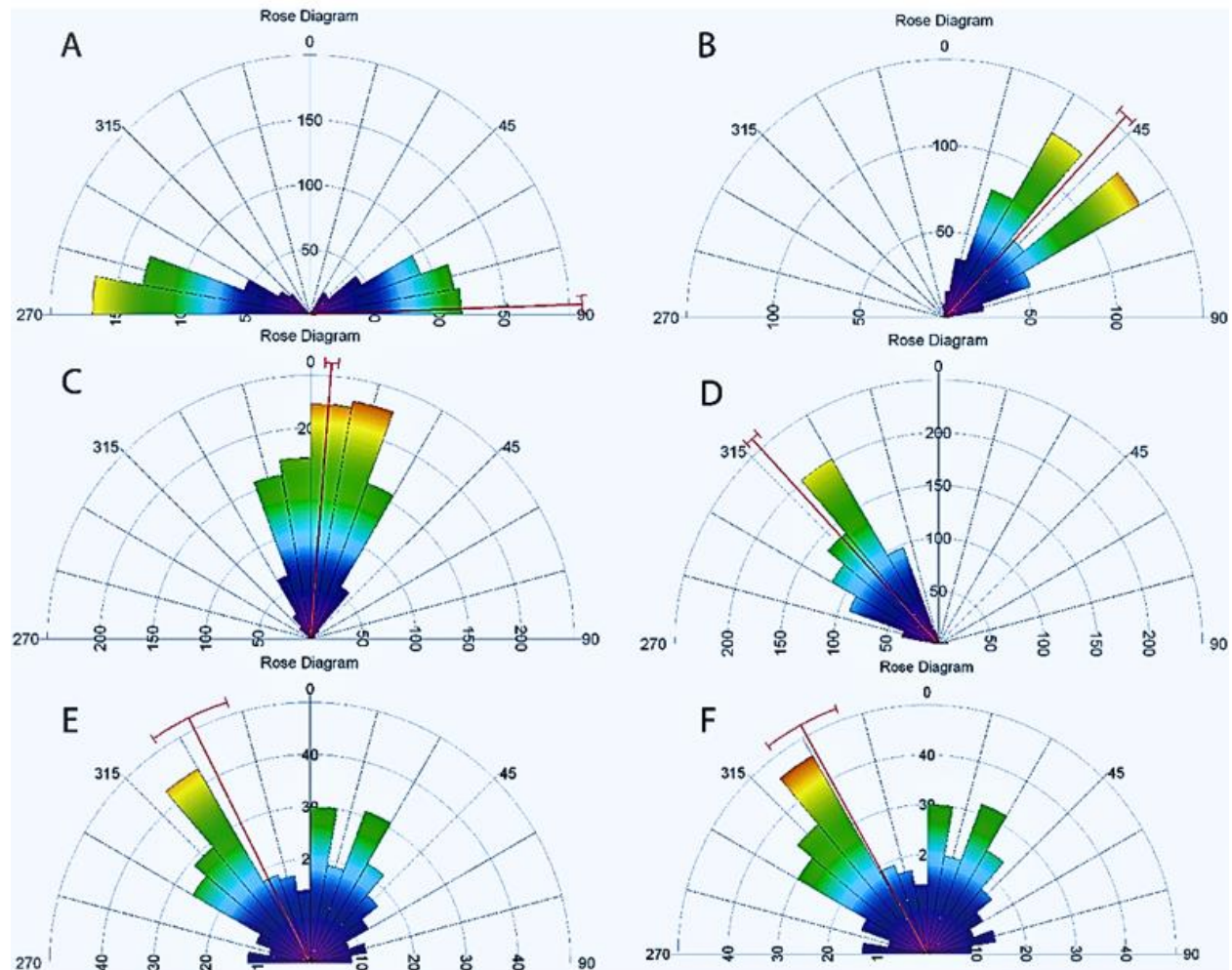


Figure 8. Directional rose diagrams of lineaments extracted A, B, C and D using each directional filter (N-S, NE-SW, E-W, NW-SE), E, combined filters, and, F, PCA extraction.

The analysis of lineament length (Figure 9) provides additional information. The majority of structures (approximately 60%) have a length between 501 and 1000 meters. It is particularly notable that the longest lineaments, those exceeding 1500 meters, belong almost exclusively to the NE-SW and

NW-SE families. This observation strongly suggests that these large-scale lineaments correspond to the surface expression of major and deep tectonic features, while shorter lineaments may represent secondary or more localized fracturing.

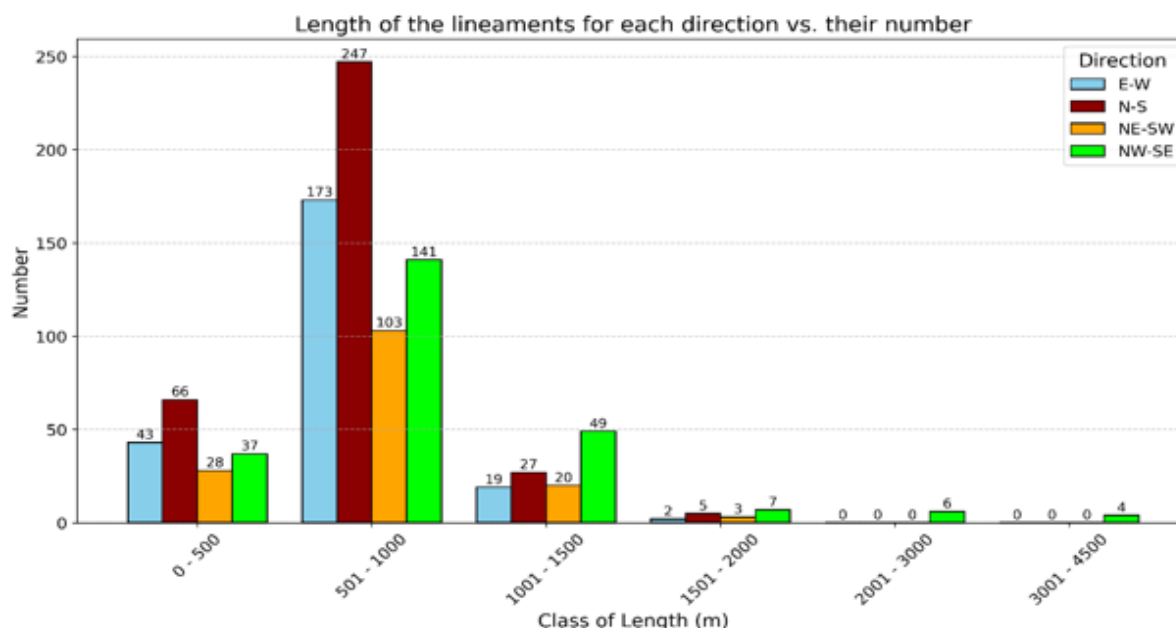


Figure 9.
Histogram of lineament length versus frequency by orientation (NE–SW, E–W, N–S, NW–SE).

3.2. Aquifer Geometry and Structural Control

The correlation of drilling data, as detailed in the methodology (section 2.4), allowed us to move from 2D surface observation to a 3D understanding of the aquifer's geometry. The correlation sections (Figure 6) explicitly illustrate the impact of the fault network on the morphology of the Jurassic reservoir.

The NE-SW section (Figure 6A), which follows the main axis of the basin, is the most revealing. It shows that the thickness of the Jurassic aquifer is not uniform. It reaches its maximum, 180 meters, at borehole 1757/21. This area corresponds to a depocenter, i.e., the point of maximum basin subsidence. On either side of this point, the thickness gradually decreases, reaching only 78 meters at borehole 1078/22, located near the Timelouka fault.

NW-SE and NNW-SSE cross-sections (Figure 6B and 6C) confirm this tectonic control. They clearly show a “stair-step” layout, with major faults (Agourai, Lemnakher, Timelouka, Adarouch) delimiting tilted blocks. These NE-SW-trending faults have caused the collapse of certain compartments (grabens) and the relative elevation of others (horsts). The Jurassic aquifer is logically thicker in the grabens, where more space was available for sedimentation (accommodation). This architecture confirms that Jurassic syn-sedimentary tectonics, controlled by NE-SW faults, is the dominant factor that dictated the final geometry of the aquifer.

4. Discussion

The results of this study unequivocally demonstrate that the geometry of the Jurassic aquifer in Agourai is primarily controlled by the NE-SW and E-W fault systems. Our approach, combining remote sensing and drilling data, allowed us to move from a simple lineament mapping to a conceptual hydrogeological model.

The predominance of NE-SW directions is consistent with previous work on Atlasic tectonics [2, 6, 14]. However, our study goes further by quantifying the impact of these faults on aquifer thickness (from 78 m to 180 m), a correlation that had not been established before in this region. Our conclusions align with studies conducted in similar contexts in Morocco, where integrated approaches combining remote sensing and GIS have also proven effective for modeling fractured aquifers [15]. The strong spatial correlation between lineament density and fractured aquifer productivity confirms similar observations in other semi-arid regions [16, 17].

The major hydrogeological implication is that areas of greater aquifer thickness (and thus greater storage potential) are located in the collapsed compartments (grabens) delimited by NE-SW faults. These faults are not only boundaries but also preferential drains that promote water recharge and circulation. The lineament map (Fig. 7) thus becomes a map of hydrogeological potential.

It is important to acknowledge the limitations of our approach. The 15 m resolution does not allow for the detection of smaller-scale fracture networks, which can nevertheless play a local role in permeability. Furthermore, the model is dependent on drilling density. To refine this work, future studies should integrate geophysical methods (such as electrical resistivity tomography) or even radar data (SAR), which have proved effective for lineament extraction in other semi-arid contexts [18].

5. Conclusion

This study successfully demonstrated the effectiveness of an integrated approach, combining remote sensing and drilling data, to elucidate the complex relationship between surface tectonics and the geometry of a deep aquifer in the Tabular Middle Atlas. The structural framework of the Agourai region is dominated by two major fault systems, oriented NE-SW and E-W, which were precisely mapped through lineament analysis. There is a direct and quantitative correlation between these tectonic structures and the geometry of the Jurassic aquifer. The faults controlled subsidence during the Jurassic, creating a horst and graben architecture that dictates the variations in reservoir thickness (from 78 m to 180 m). The originality of this study lies in this demonstration, which provides a predictive hydrogeological model for a region where this relationship had not been formally established.

Ultimately, this work not only provides a map of fracking, but also a powerful methodological tool for sustainable water resource management. It enables us to scientifically target areas with the highest aquifer potential, thus optimizing future exploration campaigns in similar semi-arid contexts.

Transparency:

The authors confirm that the manuscript is an honest, accurate, and transparent account of the study; that no vital features of the study have been omitted; and that any discrepancies from the study as planned have been explained. This study followed all ethical practices during writing.

Copyright:

© 2025 by the authors. This open-access article is distributed under the terms and conditions of the Creative Commons Attribution (CC BY) license (<https://creativecommons.org/licenses/by/4.0/>).

Références

- [1] A. Michard, "Elements of Moroccan geology," *Notes and Memoirs of the Geological Service of Morocco*, vol. 252, pp. 1–408, 1976.
- [2] D. Frizon de Lamotte *et al.*, "The Atlas system and the geodynamics of the western Mediterranean: Geological constraints," *Tectonophysics*, vol. 357, no. 1–4, pp. 1–28, 2000.
- [3] K. El-Hassani, "Structural and lithological controls on the hydrodynamics of the Turonian aquifer in the Tabular Middle Atlas: Insights from geophysical and hydrochemical data," *Hydrogeology Journal*, vol. 29, pp. 1125–1142, 2021.
- [4] H. Hollard, "The Hercynian domain of Morocco: Assessment and perspectives," *Notes and Memoirs of the Geological Service of Morocco*, vol. 314, pp. 1–275, 1985.
- [5] E. Laville, A. Piqué, M. Amrhar, and M. Bouabdelli, *Structures and tectonic evolution of Morocco. In Geology of Morocco (Notes and Memoirs of the Geological Service of Morocco)*. Rabat, Morocco: Geological Service of Morocco, 2004.

- [6] A. Piqué and A. Michard, *Moroccan hercynides: A synopsis. In The Paleozoic of Morocco Lecture Notes in Earth Sciences*. Berlin, Heidelberg: Springer, 1989.
- [7] F. F. Sabins, "Remote sensing for mineral exploration," *Ore Geology Reviews*, vol. 14, no. 3–4, pp. 157–183, 1999.
- [8] J. R. Jensen, *Remote sensing of the environment: An earth resource perspective*, 2nd ed. Upper Saddle River, NJ: Pearson Prentice Hall, 2007.
- [9] C. Pohl and J. L. Van Genderen, "Review article Multisensor image fusion in remote sensing: Concepts, methods and applications," *International Journal of Remote Sensing*, vol. 19, no. 5, pp. 823–854, 1998.
<https://doi.org/10.1080/014311698215748>
- [10] A. Singh and A. Harrison, "Standardized principal components," *International Journal of Remote Sensing*, vol. 6, no. 6, pp. 883–896, 1985.
- [11] K. Koike, S. Nagano, and M. Ohmi, "Lineament analysis of satellite images using a segment tracing algorithm (STA)," *Computers & Geosciences*, vol. 21, no. 1, pp. 109–123, 1995.
- [12] H. M. Rajesh, "Lineament mapping and analysis using Landsat ETM+ data: A case study from South India," *International Journal of Applied Earth Observation and Geoinformation*, vol. 6, no. 1, pp. 53–62, 2004.
- [13] O. Drâa, L. Aït Brahim, and S. Boutaleb, "Structural control of groundwater flow in fractured carbonate aquifers: A case study from the Middle Atlas, Morocco," *Arabian Journal of Geosciences*, vol. 14, p. 1253, 2021.
- [14] A. Mabrouki, L. Aït Brahim, and A. Michard, "The role of inherited Hercynian structures in the tectonic evolution of the Middle Atlas," *Geodinamica Acta*, vol. 32, no. 1, pp. 27–45, 2020.
- [15] F. Allali and R. Ben-Slimane, "A GIS-based multi-criteria analysis for groundwater potential mapping in the fractured carbonate aquifers of the Saïss Basin, Morocco," *Journal of African Earth Sciences*, vol. 188, p. 104532, 2022.
- [16] Y. Hamed and M. Gueddari, "Karst aquifer hydrodynamic behavior in semi-arid region: The case of Amdoun-Jebel Ichkeul, northern Tunisia," *Hydrological Sciences Journal*, vol. 54, no. 5, pp. 993–1005, 2009.
- [17] M. Jalil and M. Yassine, "Groundwater resource management in the Middle Atlas (Morocco): Issues and approaches," *Water Science and Technology Review*, vol. 23, no. 2, pp. 159–174, 2010.
- [18] S. Ziani and L. Gourari, "Integrating Landsat 8 OLI and Sentinel-1 SAR data for enhanced lineament extraction and its implication for groundwater targeting in semi-arid environments," *Remote Sensing in Earth Systems Sciences*, vol. 6, pp. 245–260, 2023.